

Extra Dimension Searches at Accelerators

T. S. Berry

University of Liverpool, Liverpool, L69 7ZE, UK

This lecture describes searches for extra dimensions conducted at accelerator facilities located throughout the world. It highlights the different approaches taken and search techniques used by the experiments. The lecture concludes with the reaches predicted to be attainable in the future.

1. INTRODUCTION

This lecture addresses the following questions: Why search for extra dimensions, what is the motivation for extra dimensional models and what models are being searched for? How are extra dimensions detectable at accelerators? What are the search signatures? Where are searches being performed? What searches are being performed and in which search channels? What are the results^a? What are the future prospects?

2. EXTRA DIMENSIONAL MODELS

There are several different extra dimensional models. The first models were introduced to address the hierarchy problem: why the electroweak scale (1 TeV) is much smaller than the Planck scale (10^{19} GeV). Presently, there are three extra dimensional models popular in accelerator new physics searches: the ADD model, named after its inventors Arkani-Hamed, Dimopoulos and Dvali [1]; the RS model, proposed by Lisa Randall and Raman Sundrum [2]; and TeV-1 size extra dimensions introduced by Antoniadis [3].

The ADD model has many large compactified extra dimensions, in which gravity can propagate. In contrast, the Standard Model (SM) particles are confined to a brane within the extra dimensions. In this model, the effective ($M_{\text{Pl}(4+n)}$) and the original Planck scale (M_{Pl}) are related by the equation $M_{\text{Pl}}^2 \sim R^n M_{\text{Pl}(4+n)}^{(2+n)}$. Whilst keeping the Planck scale constant, the effective Planck scale can be reduced to the order of a TeV, if the size of the extra dimensions is large. (Assuming toroidal shaped extra dimensions: $R \sim 10^{(30/n-19)}$ m, so for $n \geq 2$, $R < 1\text{mm}$.) In contrast, in the RS model, the hierarchy is solved by having a single highly curved (warped) extra dimension. In this scenario, gravity is localized on one brane in the extra dimension, and the SM particles are located on another. The scale of new phenomena (Λ_π), in this model, are related to the Planck scale via the equation: $\Lambda_\pi = M_{\text{Pl}} e^{-kRc\pi}$. Therefore, Λ_π can be reduced to ~ 1 TeV, if the curvature of this extra dimension is such that $kRc \sim 11-12$. The third model covered in this lecture is the TeV⁻¹ size extra dimensional model. In this model the SM chiral fermions are confined to a brane or branes, but the SM gauge bosons (W, Z, γ and g) can propagate into the extra dimensions. All of these models are potentially detectable at accelerators and have different search signatures.

^a The search results are ordered according to their signatures.

3. EXTRA DIMENSIONAL SEARCH SIGNATURES

3.1. ADD Model

In the ADD model there are two ways in which the graviton can be detected: via direct graviton emission in association with a vector-boson or via virtual graviton exchange. In the first case, the graviton would be emitted into the extra dimensions, and so would escape detection in the detector. Its existence would be deducible by missing transverse energy. The signature would therefore be missing transverse energy accompanied by a jet(s) or vector boson. The cross-section for this process depends on the number of extra dimensions. Virtual graviton exchange would result in, and therefore could be detected by, deviations in dilepton and diboson cross-sections and asymmetries from those expected from SM processes. For example, in the dilepton channel at the Tevatron, graviton exchange would not only result in the additional $q\bar{q} \rightarrow G \rightarrow l^+l^-$ process, but also a $gg \rightarrow G \rightarrow l^+l^-$, which is not present in the SM. In the ADD model graviton exchange, a broad change in cross-section at large invariant mass is expected, due to the summation over the closely spaced Kaluza-Klein (KK) towers of the graviton. The cross-section is independent of the number of extra dimensions in the Hewett convention [4]. There are two new parameters introduced in the model: M_s , the string scale and λ , a dimensionless parameter ± 1 (+1 for destructive interference and -1 for constructive interference).

3.2. RS Model

The RS model is also detectable via virtual graviton exchange and could be detected by an excess in the dilepton, dijet or diboson channel. The branching fractions for the graviton decay are shown on the left of Figure 1 [5]. The branching fraction to photons is twice that to electrons, due to the combination of spin factors (vectors for photons, spin $\frac{1}{2}$ for electrons) and the fact that photons are identical particles. The signature in this case would be a narrow resonance or series of resonances, rather than a broad change in cross-section, since the KK excitations can be excited individually on resonance, as illustrated on the right of Figure 1 [6]. The invariant mass (m_l) and the width (Γ_l) of the first resonance are determined by the parameters of the model: $\Lambda_\pi = m_l M_{Pl} / kx_1$, where the width depends on the ratio k/M_{Pl} : $\Gamma_l = \rho m_l x_1^2 (k/M_{Pl})^2$. The resonances are predicted to be separated by the characteristic Bessel function separation, where $m_n = kx_n e^{krc\pi} (J_1(x_n)=0)$ [6].

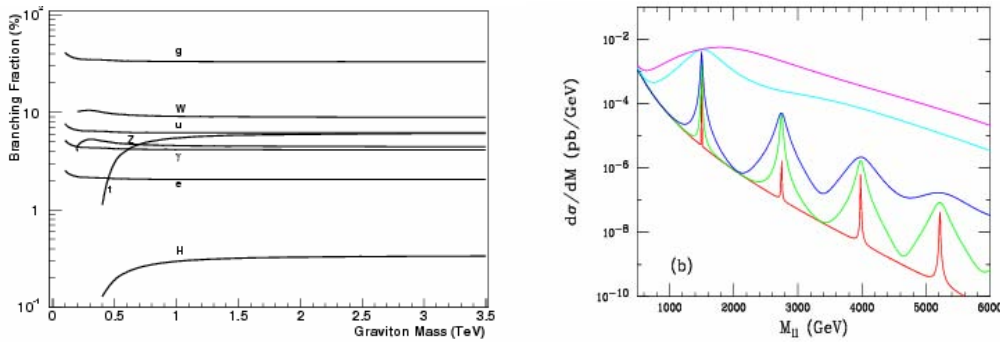


Figure 1: Right: Graviton branching fractions in the RS model [5]. Left: Drell-Yan production of a 1500 GeV KK graviton and its subsequent tower states at the LHC. From top to bottom, the curves are for $k/M_{Pl} = 1, 0.5, 0.1, 0.05$, and 0.01 , respectively [6].

3.3. TeV^{-1} Size Model

In the TeV^{-1} size extra dimensional models considered only fermions are confined to a brane within the extra dimensions, whereas the gauge fields can propagate into the extra dimensions. Consequently, this results in KK excitations of the gauge bosons [7]. From the four-dimensional point of view the masses of the SM gauge bosons (M_0) which propagate in the extra dimensions are equivalent to towers of KK states with masses (M_n) described by $\sqrt{(M_0^2 + n^2 M_C^2)}$, where M_0 is the mass of the SM gauge boson, M_C corresponds to the compactification scale (where R is the size of the compact dimension ($R = M_C^{-1}$)) and $n=1,2,\dots$. The KK states of the W , Z , γ and g bosons are detectable via both direct production and virtual effects. For example, there is mixing among the zeroth (SM gauge boson) and the n^{th} modes ($n=1,2,3,\dots$) of the W and Z bosons, since the entire tower of KK states have the same quantum numbers as their zeroth state gauge boson. In the models discussed here, one (M1) assumes that all of the SM fermions are located at the same orbifold point and the other (M2) assumes that the quarks and leptons are located at opposite fixed points in the orbifold [7]. Figure 2 shows the invariant mass distribution of e^+e^- pairs for the SM (full line) and that expected for model M1 (dashed line) and M2 (dotted line) for a mass of the lowest lying KK excitation of 4 TeV [7]. There are two noticeable features: the peak centered around M_C , corresponding to superposition of the $\gamma^{(1)}$ and $Z^{(1)}$ and, for model M1, a suppression of the cross-section with respect to the SM for masses below the resonance. This suppression is due to the negative interference terms between the SM gauge bosons and the whole tower of KK excitations, which is sizable even for M_C well above the ones accessible to a direct detection of the mass peak. This shape is the consequence of the model choices requiring both the leptons and the quarks to be at the same orbifold point (M1), whereas model M2 yields an enhancement of the off peak cross-section.

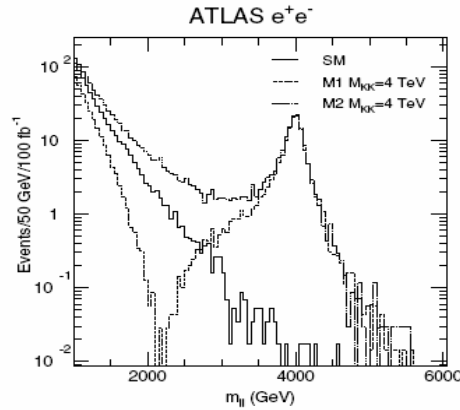


Figure 2 : Invariant mass distribution of e^+e^- pairs predicted in the TeV^{-1} size extra dimensional model for the Standard Model (full line) and for model M1 (dashed line) and M2 (dotted line), in which the mass of the lowest lying KK excitation is 400 TeV. The histograms are normalized to 100 fb^{-1} [7].

4. ACCELERATOR SEARCH FACILITIES

Searches for extra dimensions have been and are being conducted throughout the world at various high energy collider facilities: Tevatron at Fermilab in the USA [8]; HERA at DESY, Hamburg [9] and LEP at CERN, Geneva [10]. The Tevatron (Run II) collides protons onto antiprotons at the centre-of-mass energy of 1.96 TeV within the CDF and D0 detectors (Run I operated at 1.8 TeV). It is presently the highest energy collider presently operating in the world.

HERA is currently the world's only electron-proton collider. It collides 27.5 GeV electrons on to 920 (820) GeV protons. These intersect at collision points inside the H1 and ZEUS detector. CERN is, at present, the world's largest particle physics laboratory. It hosted LEP, an electron-positron collider, which operated initially a centre-of-mass energy of 91 GeV (LEP I) and subsequently in the range from 136 to 208 GeV (LEP II). There were four detectors located around the LEP ring: ALEPH, DELPHI, L3 and OPAL. The LEP ring has now been superseded by the construction of the Large Hadron Collider (LHC) and its detectors: ALICE, ATLAS, CMS and LHCb. The LHC is to be a 14 TeV centre-of-mass energy proton-proton collider. First collisions are scheduled to occur in 2007.

5. EXTRA DIMENSIONAL SEARCHES OVERVIEW

Table 1 summarizes the search signature, channel and the experiment at which searches for extra dimensional models have been performed.

Table 1: Summary of the search signature, channel and the experiment at which searches for extra dimensional models have been performed.

Signature	Channel	Experiment	Model
Graviton Emission	γ +MET	LEP, CDF	ADD
	jets+MET	CDF, D0	
Graviton Exchange	$\mu\mu$	CDF, D0	ADD, RS
	ee	CDF, D0	
	ee+ $\gamma\gamma$	D0	
	$\gamma\gamma$	CDF	
	$e^{+/-}X$	H1	ADD
Boson Exchange	ee	D0	TeV^{-1}

6. GRAVITON EMISSION

6.1. Photon Plus Missing Transverse Energy

One way to detect the ADD model extra dimensions is to look for evidence of graviton emission. Since the graviton escapes detection as it goes into the extra dimensions, the result would be an enhanced rate of photon or jet(s) plus missing transverse energy events (γ +MET, jet(s)+MET). Searches in the γ +MET channel were conducted at LEP and searches for both of these signatures have been performed by CDF and D0 at the Tevatron.

The Feynman diagrams for $e^+e^- \rightarrow \gamma G$, searched for at LEP are illustrated in Figure 3. The differential cross-section for this process depends on the gravity scale (M_D) and on the number of extra dimensions. It increases rapidly at low photon energies and angles, as illustrated on the left of Figure 4, in which x_γ is the ratio of the γ energy to the beam energy and θ_γ is the polar angle of the γ relative to beam line.

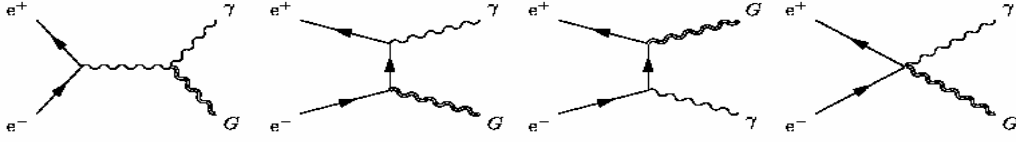


Figure 3: Feynman diagrams for the process $e^+e^- \rightarrow \gamma G$, used at LEP to search for evidence of ADD model extra dimensions via graviton emission. The diagram on the left shows s-channel exchange, the central diagrams illustrate t-channel exchange and the one of the right illustrates a four-particle contact interaction.

Searches made at three of the LEP experiments: ALEPH, DELPHI and L3 were combined [11]. The datasets used were collected when LEP was operating at a centre-of-mass energy of (\sqrt{s}) 189-208 GeV from 1998 to 2000. This corresponds to about 0.6 fb^{-1} per experiment, equating to a total luminosity of 1.9 fb^{-1} . The search selection used to identify the photon required one cluster in the electromagnetic calorimeter with no matching charged track and a transverse momentum in the range $0.02\sqrt{s}$ to $0.04\sqrt{s}$. Also it was specified that there be no other significant detector activity. The principal irreducible background in this search is from $e^+e^- \rightarrow \nu\bar{\nu}\gamma$. The other main background, in the region in which the photon has low transverse momentum, is from $e^+e^- \rightarrow e^+e^-\gamma(\gamma)$. Here, the background is enhanced due to events in which both of the electrons have low momentum and cannot be detected. The data observed by all of the experiments showed good agreement with the SM predictions. The combined L3 and DELPHI distribution of events as a function of the photon energy/beam energy is shown on the right of Figure 4. Lower limits on the gravity scale were derived individually by each experiment a function of number of extra dimensions (n), and subsequently the results combined. Table 2 summarises the combined results and these are illustrated in Figure 5.

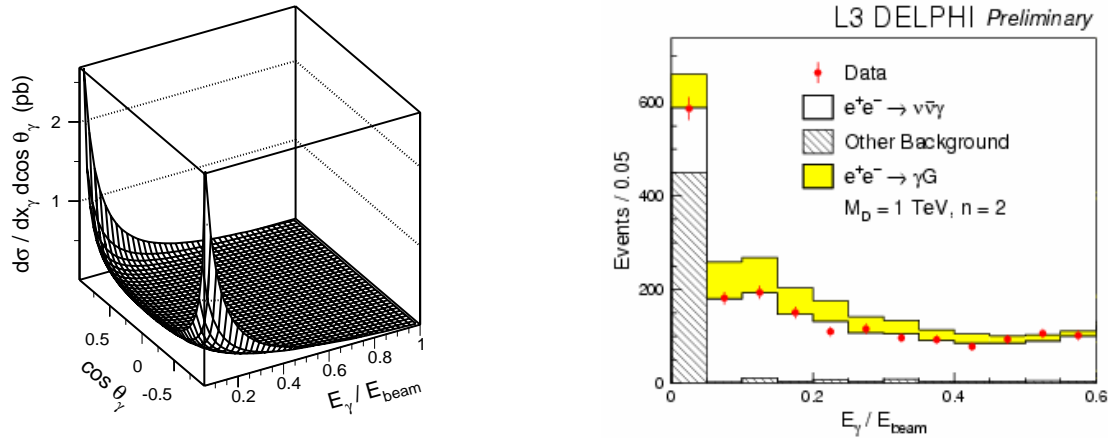


Figure 4: Left: The differential cross-section of $e^+e^- \rightarrow \gamma G$ events. Right: The combined L3 and DELPHI distribution of events as a function of the photon energy/beam energy [11].

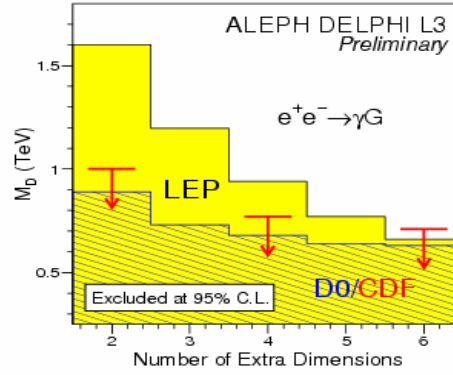


Figure 5: Limits on the gravitational scale (M_D) as a function of the number of extra dimensions in the ADD model obtained by the combination of LEP experiment results (ALEPH, DELPHI and L3) for searches in the $e^+e^- \rightarrow \gamma G$ channel (1.9 fb^{-1}). Also shown are CDF (arrows) and D0 (hatched) jet+MET graviton emission results [11].

Table 2: Table of the limits on the gravitational scale (M_D) and the radius of the extra dimensions (R) as a function of the number of extra dimensions (n) in the ADD model obtained by the combined experimental results for $e^+e^- \rightarrow \gamma G$ from ALEPH, DELPHI and L3 at LEP [11].

n	M_D (TeV)	R (mm)
2	> 1.60	< 0.19
3	> 1.20	$< 2.6 \times 10^{-6}$
4	> 0.94	$< 1.1 \times 10^{-8}$
5	> 0.77	$< 4.1 \times 10^{-10}$
6	> 0.66	$< 4.6 \times 10^{-11}$

CDF performed a similar search for graviton emission in the photon plus missing transverse energy channel using 87 pb^{-1} of Run I data [12]. The Feynman diagrams for this process are shown in Figure 6. The search selection required one photon with transverse energy greater than 55 GeV in the central region of their detector ($|\eta| < 1$)^a and the event to have a missing transverse energy greater than 45 GeV. Events with jets with transverse energy greater than 15 GeV and/or tracks with transverse momentum greater than 5 GeV were rejected. The main backgrounds to the search were from cosmic ray muons: 6.3 ± 2.0 ; $Z^0 \gamma \rightarrow \nu \nu \gamma$: 3.2 ± 1.0 ; $W \rightarrow e \nu$ (“ $\gamma \nu$ ”) where the electron was misidentified as a photon: 0.9 ± 0.1 ; prompt diphotons: 0.4 ± 0.1 and $W \gamma$ ($\gamma \nu$) where the electron was not detected: 0.3 ± 0.1 . The observed 11 events are consistent with SM prediction of 11.0 ± 2.3 events. Limits were set on the gravitational scale: $M_D > 0.55 \text{ TeV}$ for $n=4$, $M_D > 0.58 \text{ TeV}$ for $n=6$ and $M_D > 0.60 \text{ TeV}$ for $n=8$. These limits are not as restrictive as those obtained by the LEP experiments.

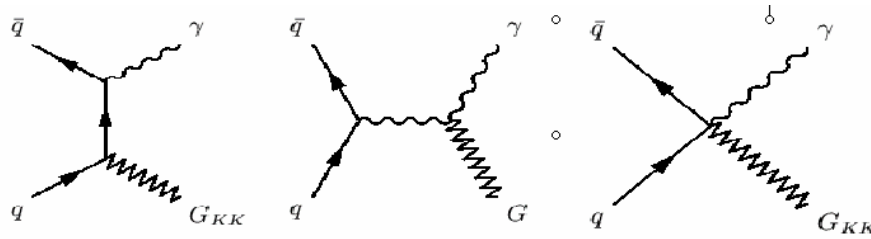


Figure 6: Feynman diagrams the graviton emission searched for at the Tevatron ($pp\text{-}\bar{p} \rightarrow \gamma G$).

6.2. Jet(s) + Missing Transverse Energy

At the Tevatron, more constraining limits on the ADD model from graviton emission come from the jets plus missing transverse energy searches ($pp\text{-}\bar{p} \rightarrow \text{jet(s)} + G$). The Feynman diagrams for the three sub-processes for this interaction: $gq\text{-}\bar{q}$, qg and gg and their cross-sections as a function of the transverse momentum of the jet at the Tevatron are shown in Figure 7 [13]. The relative contribution from each sub-process depends on the number of extra dimensions. For $n > 2$, $gq\text{-}\bar{q}$ is the dominate process. The cross-sections for all of the sub-processes fall as $1/M_D^{(n+2)}$.

The search selection used at CDF required a jet in the central region of the detector with transverse energy greater or equal to 80 GeV and a missing transverse energy in the event of greater than 80 GeV. A second jet was allowed if its transverse energy was greater than 30 GeV. Additionally, the event was required to contain no isolated tracks with transverse momentum greater or equal to 10 GeV. The main background in this analysis channel is from irreducible $Z(\nu\nu\rightarrow)\text{jets}$, as is illustrated in the missing transverse energy distribution shown in Figure 8 [14]. Other backgrounds include $W(\nu\tau\rightarrow)\text{jets}$. 284 events were observed compared to 274 ± 16 expected. Limits were set on the gravitational scale: $M_D > 0.77$ TeV for $n=4$ and $M_D > 0.73$ TeV for $n=6$. D0 have also performed searches for graviton emission searching for monojet plus missing transverse energy in both Run I and Run II data, however, at present their limits are not as restrictive as CDF's [15,16]. This is indicated on the left of Figure 8.

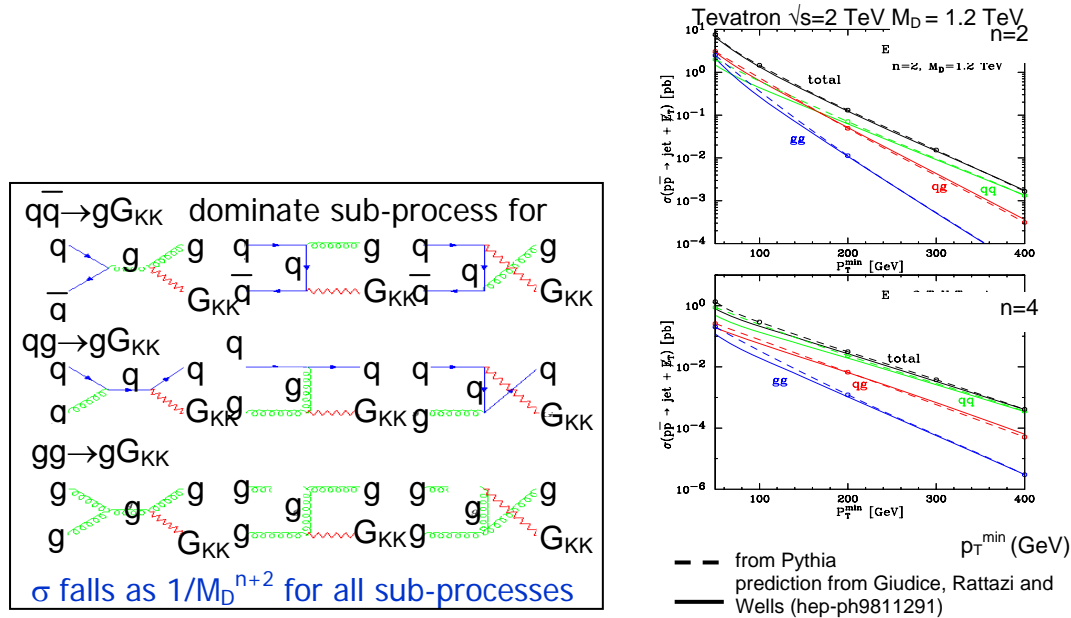


Figure 7: Left: Feynman diagrams for the three sub-processes $pp\text{-}\bar{p} \rightarrow \gamma G$: $gq\text{-}\bar{q}$, qg and gg initiated. Right: Their cross-sections as a function of the transverse momentum of the jet at the Tevatron [13].

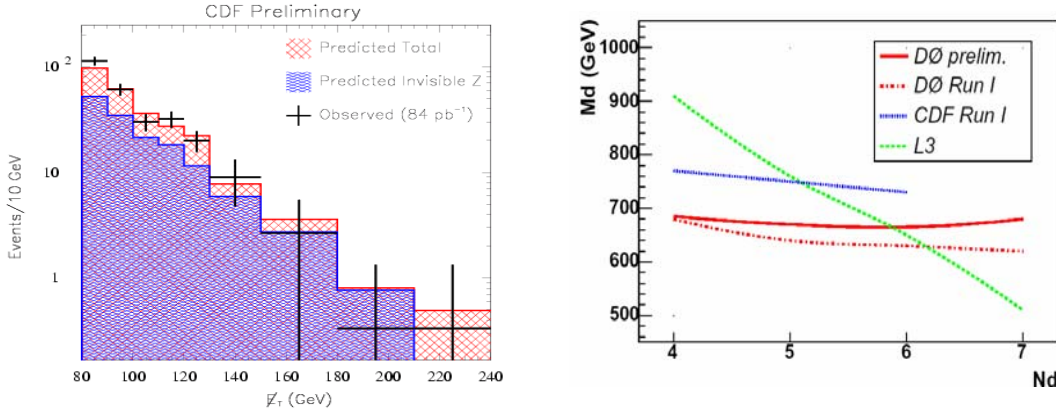


Figure 8: Left: Missing transverse energy distribution in the CDF graviton emission search in the jet(s) plus missing transverse energy channel (84 pb^{-1} of Run I data). Right: Comparison of the limits on the gravitational scale (M_D) as a function of the number of extra dimensions obtained by D0 in Run I (79 pb^{-1}), Run II (85 pb^{-1}), CDF Run I (84 pb^{-1}) in the jet(s)+MET channel and L3 results for γ +MET channel ($\sim 0.6 \text{ fb}^{-1}$).

6.3. Summary of Graviton Emission ADD Model Limits

The LEP and Tevatron graviton emission results are complementary. For less than 6 extra dimensions (n), the LEP limits are the most restrictive using the γ +MET channel as shown in Figure 5. This LEP search is cleaner and has lower backgrounds than jet(s)+MET search performed at the Tevatron, so the precision of their experiments dominates for lower values of n . For larger numbers of extra dimensions ($n > 6$), the Tevatron limits are better from the jet(s)+MET channel. This is because of the higher energy available at the Tevatron, which has a bigger effect at larger values of n . This can be explained by the fact that the cross-section (σ) is proportional to the total number of accessible modes in the KK tower (N_{KK}), which is proportional to the centre-of-mass energy available \sqrt{s} : $\sigma \propto N_{KK} \propto \sqrt{s}$. This is true for each extra dimension, so the total cross-section $\sigma_T \propto (\sqrt{s})^n$. Therefore, the difference in energy has a bigger effect for $n=6$ than $n=2$, as illustrated in Figure 5.

7. GRAVITON EXCHANGE

Searches for graviton exchange at accelerators are sensitive to both the RS and the ADD extra dimensional models and searches are performed in several different channels. There are similarities and distinct features in the search strategies used at different accelerators and for the two models. The similarities include the search channels. The accelerators search for deviations in (ee , $\mu\mu$, $\gamma\gamma$) cross-sections (σ) and angular distributions from SM processes caused by graviton exchange. If a deviation were observed, the origin of the new physics could potentially be determined by

the nature of the deviation. The RS model could be distinguished from the ADD model, by the observation of a resonance, in contrast to a broad change in cross-section. The spin two property of the graviton could be used to distinguish an extra dimensional resonance from other new physics, such a Z' boson, which could look like the first resonance in the RS model.

The advantage of the searching in the dielectron and dimuon channel at hadron colliders is the comparatively clean experimental signature, low background and the Z^0 peak can be used as a calibration point. The diphoton channel has the advantage that it has a branching ratio of twice that to dielectrons or dimuons. The Feynman diagrams for the SM processes and graviton exchange for dilepton and diphoton production are shown in Figure 9.

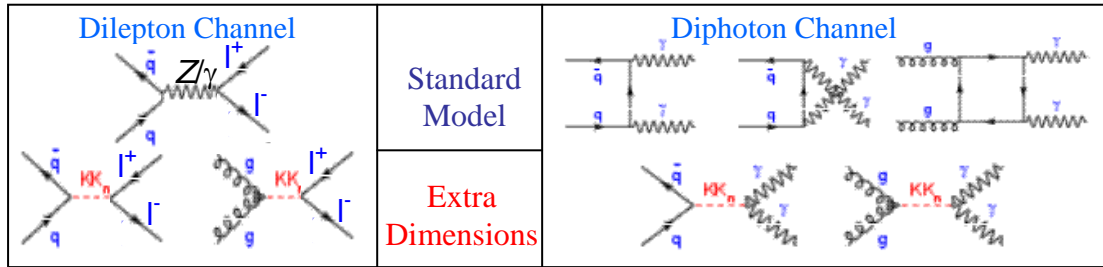


Figure 9: Feynman diagrams for the SM processes and graviton exchange dilepton and diphoton production, for the RS and ADD extra dimensional models.

The two detectors on the Tevatron ring use different strategies to search for graviton exchange. CDF perform signature based searches, in which they compare the data invariant mass spectrum to the expected SM distribution [17]. They determine the acceptance as a function of spin and use this to obtain spin dependent cross-section times branching ratios ($\sigma \cdot BR$ s). They then interpret the same datasamples for different spin scenarios and set limits on many new models. For example, the same dielectron and dimuon datasets are used to set limits on spin 0: RPV sneutrinos; spin 1: Z' , Technicolor ρ , ω ; and spin-2: RS model gravitons and ADD model gravitons. CDF also study the angular distributions independently, but these are not used in determining the limits. In contrast, D0 use a different search strategy [18,19,20]. They perform more extra dimensional specific searches and optimise for the specific search. Since the graviton couples to both electrons and photons (see the right of Figure 1), D0 combine their dielectron and diphoton datasets at the selection level to maximise reconstruction efficiency. This is productive because of the criteria used to identify electrons and photons. They both deposit energy in the electromagnetic calorimeter and so are called electromagnetic objects. However, photons are uncharged, so in contrast to electrons, leave no track in the tracking chamber, therefore photon identification specifies there be no track. However, if a photon converts (i.e. decays to two electrons) then will be at least one track from the decay electrons (assuming at least one of the electron tracks is reconstructed) and the photon would consequently not be identified. Standard electron identification requires a track, but due to imperfect track reconstruction or cracks in the detector then the track can be lost. In this case the electron would not be identified. In addition, D0 perform three-dimensional, rather than one-dimensional, fits in invariant mass and angular distribution.

7.1. ADD Model

7.1.1. Tevatron's Dielectron And Diphoton ADD Model Searches

The D0 ADD model search used 200 pb^{-1} of Run II data. Selection required two isolated electromagnetic objects with transverse energy greater than 25 GeV. One was required to be in the central electromagnetic detector and the other either in the central or in the forward electromagnetic detector. Figure 10 shows the invariant mass spectra for the data observed, the QCD background, the SM prediction and the signal prediction for a graviton of string scale $M_s = (0.3\pi)^{1/4}$ [18].

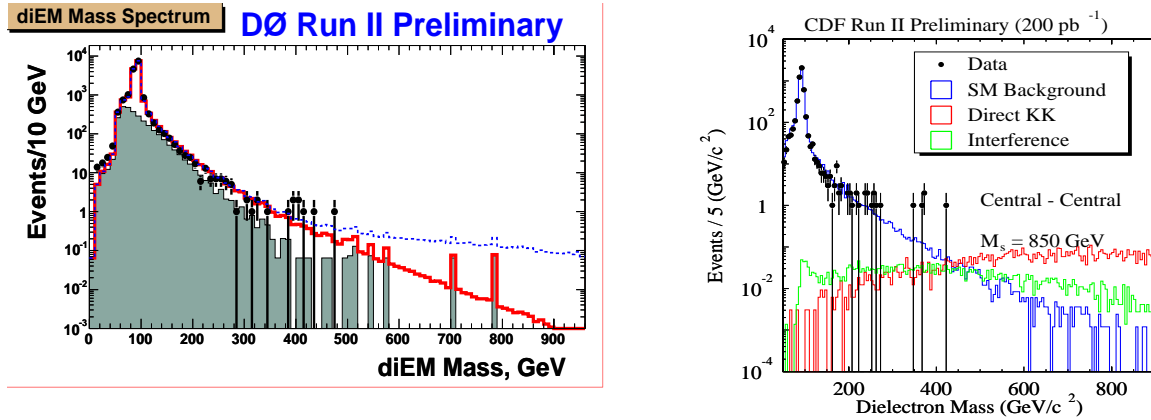


Figure 10: Left: Invariant mass spectra for the data observed (points), the QCD background (shaded), the SM prediction (solid line) and the signal prediction for a graviton of string scale $M_s = (0.3\pi)^{1/4}$ (dotted line) in D0's search for ADD model extra dimensions in 200 pb^{-1} of Run II data [18]. Right: Invariant mass distribution for the data observed and the SM background expected in CDF's search for new physics using 200 pb^{-1} of Run II data. Also shown are the direct and interference terms predicted in the ADD extra dimensional model for a string scale of $M_s = 850 \text{ GeV}$ [17].

Interestingly, there are eight events in the datasample with an invariant mass greater than 350 GeV. Six of these form a bump around 400 GeV. Hints perhaps of new physics? These events were investigated. It was concluded that they could not be caused by a $Z' \rightarrow ee$ resonance for two reasons. Firstly, all of the events have one or zero tracks, which implies at least one of the pair is a photon, which do not couple to Z' bosons. Secondly, the bump is twice as narrow as would be expected from a narrow resonance smeared with typical resolution of the D0 electromagnetic calorimeter. Intriguingly, of the two highest mass events one is a dielectron pair and the other diphoton. Also both have very high scattering angle. This makes them excellent candidates for new physics since they possess kinematics typical of a signal from large extra dimensions. These are interesting events, but consistent with the SM.

CDF perform an analogous search for the ADD model [17]. The differences being that they search in the dielectron and diphoton channel independently. They also perform fits in the invariant mass only. In the dielectron case, they search in 200 pb^{-1} of Run II data and for two isolated electrons with transverse energy greater than 25 GeV. They require one to be in the central electromagnetic detector and the other to be either in the central or in the forward electromagnetic detector. They expect 11.1 events and observe 14 for an invariant mass greater than 300 GeV, and above 350 GeV, 4.6 events are expected and 9 observed. The invariant mass distribution for the data observed and the SM background is shown on the right of Figure 10. Also shown are the direct and interference terms expected for a string scale of $M_s = 850 \text{ GeV}$.

7.1.2. Dimuon ADD Model Searches

D0 also search for the ADD extra dimensional model in the dimuon channel [19]. The search selection requires the muons to have a transverse momentum greater than 15 GeV, to have isolated tracks and the dimuon invariant mass to be greater than 50 GeV. In addition, cuts are made to reject cosmic ray muons. They expect 6.4 events and observe 5 for an invariant mass greater than 300 GeV, and above 350 GeV, 1.3 events are expected and 1 observed. Hence, no deviation from the SM expectation was observed, and limits were extracted using a fit in invariant mass and angular distribution.

7.1.3. Summary Of Graviton Exchange ADD Model Limits

Both D0 and CDF observed no significant deviation to the expected SM distributions. The ADD model 95% confidence level (C.L.) limits obtained by both experiments are summarised in Table 3. The D0 combined dielectron-diphoton Run I and Run II result is the most stringent limit on the ADD model to date.

Table 3: Summary of the 95% C.L. lower limits on fundamental Planck scale in TeV as a function of the number of extra dimensions (n) for the ADD model, obtained by CDF and D0, using different formalisms [18].

	GRW	N						Hewett
		2	3	4	5	6	7	$\lambda=\pm 1$
D0 Run II: $\mu\mu$	1.09	1.00	1.29	1.09	0.98	0.91	0.86	0.97/0.95
D0 Run II: $ee+\gamma\gamma$	1.36	1.56	1.61	1.36	1.23	1.14	1.08	1.22/1.10
D0 Run I + II: $ee+\gamma\gamma$	1.43	1.61	1.70	1.43	1.29	1.20	1.14	1.28/NA
CDF Run II: ee	1.11		1.32	1.11	1.00	0.93	0.88	0.96/0.99

7.2. RS Model

Analogously to the ADD searches, D0 perform searches for the RS model in both the dielectromagnetic and dimuon channels [20] and CDF search in the dielectron channel and also independently in the dimuon and diphoton channels [17,21].

7.2.1. D0 Dielectron and Dimuon RS Model Searches

The dielectromagnetic search required, as for the ADD model search, two isolated electromagnetic objects with transverse energy greater than 25 GeV; one in the central electromagnetic detector and the other either in the central or forward. The search used 275 pb^{-1} of Run II data. The dimuon search required two high transverse momentum muons (>15 GeV minimum ionising particles), which matched tracks in central tracking chamber and made signals in the muon drift chambers (if fiducial). An opposite charge requirement was not made, as the efficiency determination of the sign of the charge degrades at high momentum. Cosmic rays were reduced by requiring the muon arrival times at the muon detectors were consistent with those from beam collisions. The search used 246 pb^{-1} of Run II data.

Good agreement is found between data and the expected background for both search channels, as is illustrated in Figure 11. In the ADD model, a broad change in cross-section was expected, therefore templates were used to make a fit in order to extract the limit. However, in the RS model, a resonance in invariant mass spectrum is expected.

Therefore search windows rather than the whole spectrum can be used to set limits. On the left and right of Figure 11 are shown the reconstructed invariant mass of a RS model graviton resonance of mass of 300 GeV and a coupling of $k/\bar{M}_{Pl} = 0.05$ in the dielectromagnetic channel and dimuon channel respectively. The width of the resonances are different, because of the detector resolutions. For the electrons and photons the electromagnetic energy is determined using the calorimeters, whereas the muon search uses the tracker to determine the transverse momentum of the muons. Consequently, different search windows were used for the two channels. Symmetric windows with a width of six times the detector resolution were used in the electron case, in contrast to asymmetric windows with only a lower mass bound in the muon case, because of the reconstructed long high-mass tail.

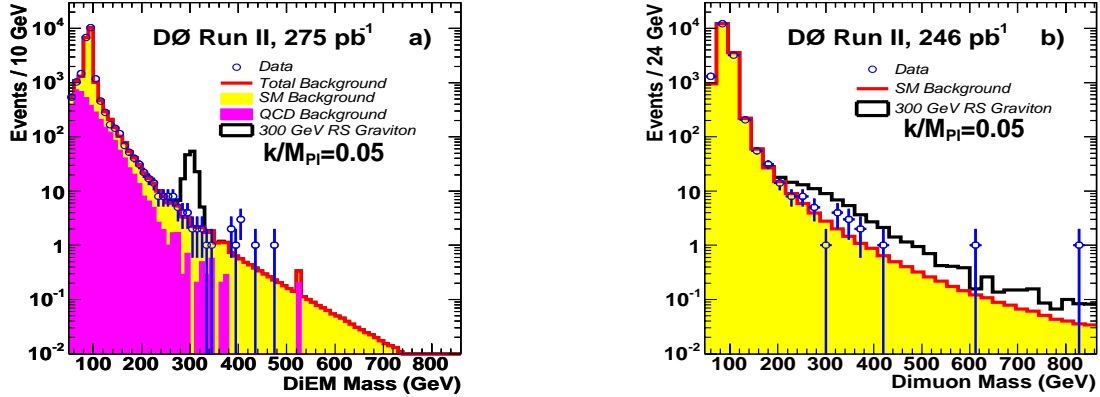


Figure 11: Invariant mass spectra for D0's RS model search in the dielectromagnetic (left) and dimuon (right) channel respectively, using Run II data. Shown in solid black is the expected reconstructed invariant mass of an RS model graviton resonance with a mass of 300 GeV and coupling of $k/\bar{M}_{Pl} = 0.05$ [20].

7.2.2. Summary Of D0's Graviton Exchange RS Model Limits

The limits for both channels and the combined result are shown in Table 4. The combined limits are slightly less restrictive than the dielectromagnetic limits, because of the overall small excess of observed events in the dimuon channel. The dielectromagnetic limits are the most restrictive limits on the RS model to date. The limits and exclusion plane are displayed in Figure 12. For a coupling of k/\bar{M}_{Pl} of 0.1 the lower mass limit obtained is 785 GeV and for 0.01, the limit is 250 GeV.

Table 4: Summary of the RS model limits obtained by D0 in their dielectromagnetic (275 pb^{-1}) and dimuon (246 pb^{-1}) channel searches. The combined results are shown in the column on the right [20].

Graviton Mass	DiEM Channel				Dimuon Channel				Combined Limit
	Window	Background	Data	Limit	Window	Background	Data	Limit	
200	190-210	51.5 ± 5.2	53	70.2	> 160	90.1 ± 11.7	96	437	70.8
300	280-320	11.1 ± 1.1	12	28.9	> 230	26.2 ± 3.4	28	178	29.0
400	380-420	2.40 ± 0.33	6	30.5	> 270	14.7 ± 1.9	17	144	30.7
700	620-780	0.30 ± 0.25	0	8.2	> 300	10.2 ± 1.3	13	117	8.7
800	700-900	0.13 ± 0.13	0	8.1	> 300	10.2 ± 1.3	13	115	8.6

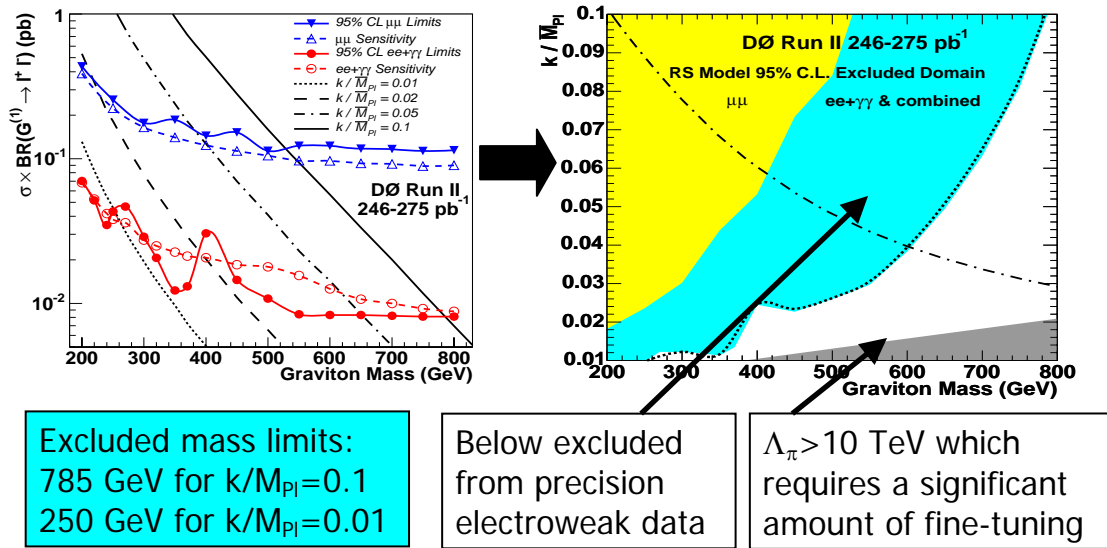


Figure 12: The RS model limits (left) and exclusion plane (right) obtained by DØ in their dielectromagnetic and dimuon channel searches. The combined result is indicated in the exclusion plane by the dotted line.

7.2.3. CDF Dielectron, Diphoton and Dimuon RS Model Searches

CDF have also performed Run II RS model searches. However, they search separately in the dielectron and diphoton channels as well as in the dimuon channel. In the electron channel, similarly to DØ, CDF require either both electrons to be in the central electromagnetic detector or one in the central and the other in the forward calorimeter. The search selection and dataset used are the same as for the ADD dielectron search, since they perform model independent searches. However, in the RS model case, CDF in Run II also study forward-forward dielectron events. This gives them an increased acceptance, and was not done in Run I. The search selection for this requires two forward electromagnetic clusters, which are isolated and have transverse momentum greater than 25 GeV. A new tracking algorithm was developed especially for forward electrons, which uses silicon tracks, because the central tracker does not cover the forward regions. Although adding forward-forward electron data increases acceptance, the background from QCD dijets is larger in the forward regions than in central. They expected 2.7 ± 0.7 events and observed 8 for an invariant mass greater than 300 GeV, and above 350 GeV, expected 1.4 ± 0.3 events and 3 observed.

In the diphoton search performed by CDF, the selection required two isolated photons in the central region of the detector, with transverse energy greater than 15 GeV. The main backgrounds in this search are from Standard Model diphoton production, which is dominant at very high masses, and the background from fake photons caused by γ -jet and jet-jet events, where the jet fragments into a hard π^0 which decays to two photons ($\pi^0 \rightarrow \gamma\gamma$). These backgrounds distribution and the data observed are shown as a function of invariant mass in Figure 13. For an invariant mass greater than 300 GeV, 4.2 ± 1.0 events were expected and 1 observed, and above 350 GeV 1.5 ± 0.5 events were expected and 1 observed.

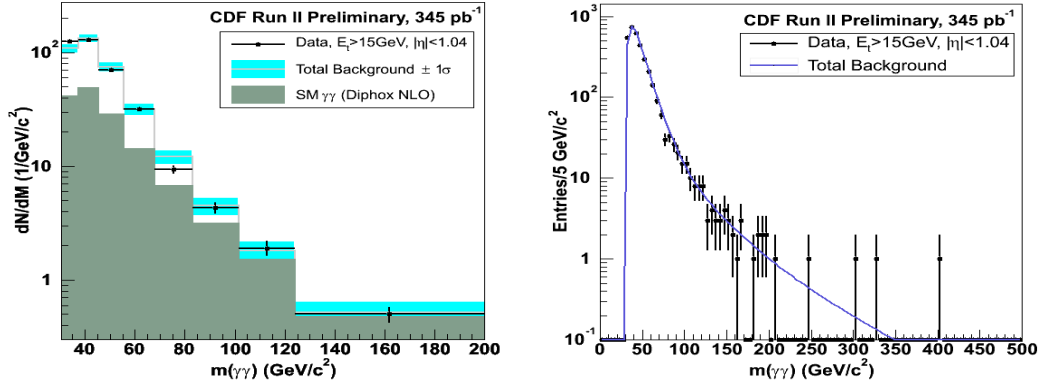


Figure 13: Diphoton data and background invariant mass spectrum obtained by CDF in their RS model search in 345 pb^{-1} Run II data.

CDF's RS model dimuon search selected two isolated muons with transverse momentum greater than 20 GeV from 200 pb^{-1} of Run II data. One muon was required to have a pseudorapidity of less than one and the second less than 1.5. In order to increase acceptance, the latter muon was not required to match a stub in the muon detectors. Cosmic rays were vetoed using track-timing cuts. For an invariant mass greater than 300 GeV, 5.2 ± 0.3 events were expected and 6 observed, and above 350 GeV 3.2 ± 0.2 events expected and 1 observed.

7.2.4. Summary of CDF's Graviton Exchange RS Model Limits

CDF set lower mass limits on the RS model graviton at the 95 % confidence level. In the diphoton channel, the method used was similar to that used in the D0 dielectromagnetic search, i.e. using one-dimensional fits in invariant mass windows around the graviton mass (M_G): CDF used $M_G \pm 3\sigma$. However, the dielectron and dimuon search used a binned likelihood method to fit the invariant mass spectra. The limits obtained are listed in Table 5 and illustrated in Figure 14. Of the three searches, the diphoton search gives the most restrictive limits. At low invariant masses, the dielectron channel has largest acceptance. However, at high masses, the diphoton channel has largest acceptance and the branching ratio for gravitons to two photons is twice that to two electrons. These RS model limits obtained by CDF are not as exclusive as those presently obtained by D0.

Table 5: Summary of the lower mass limits for the RS model graviton at the 95 % confidence level obtained by CDF in their dielectron (200 pb^{-1}), dimuon (200 pb^{-1}) and diphoton (345 pb^{-1}) searches.

Channel	Luminosity	M_G (GeV)	M_G (GeV)
ee	200	200	640
$\mu\mu$	200	170	610
ee+ $\mu\mu$	200	200	700
$\gamma\gamma$	345	220	690

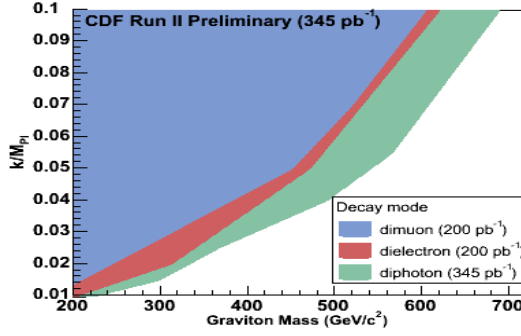


Figure 14: Exclusion plane of the RS model graviton mass and coupling obtained by CDF in their dielectron (200 pb^{-1}), dimuon (200 pb^{-1}) and diphoton (345 pb^{-1}) searches using Run II data [21].

7.3. H1 ADD Model Searches

H1 use a different search strategy, because of the very different physics environment created by eq rather than pp-bar collisions. They perform signature based searches in which measurements of the inclusive cross-sections ($e^{\pm}p \rightarrow e^{\pm}X$) over a huge range in four-momentum transfer (Q^2 , $200\text{--}3000 \text{ GeV}/c^2$) are made [22]. The data are then compared to the SM expectation. This is illustrated in Figure 15. It is at high Q^2 at which deviations due to new physics are expected to be most prominent and could indicate the presence of quark substructure or new particles. The same data is interpreted in the context of many new models. For example, limits are set on contact interactions, leptoquarks, R-parity violating squarks, and electron and quark substructure (form factor analysis).

In deep inelastic scattering, graviton exchange may contribute to the e-q sub-process, but there is also a new interaction, e-g scattering, which is not present in the SM. H1 used their neutral current cross-section measurements, with integrated luminosities of 16.4 pb^{-1} and 100.8 pb^{-1} of e^-p and e^+p data respectively to set limits on the ADD model. Figure 16 shows the limits obtained for e^-p and e^+p data in the case of constructive ($\lambda=-1$) and destructive interference ($\lambda=+1$) and also combined the results [22]. These limits are not as exclusive as the graviton exchange results obtained at the Tevatron.

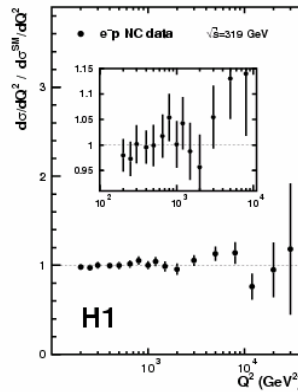


Figure 15: Cross-section ratio of data/SM at $\sqrt{s} = 319 \text{ GeV}$ for H1's measurement of the inclusive cross-sections $e^-p \rightarrow e^-X$ [22].

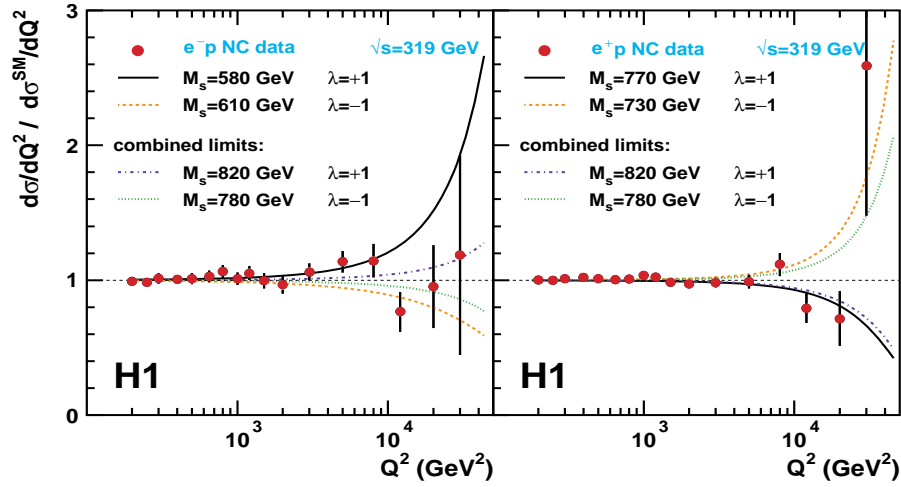


Figure 16: ADD model limits obtained by H1 using e^-p (left) and e^+p (right) data in the case of constructive ($\lambda=-1$) and destructive interference ($\lambda=+1$) [22].

8. BOSON EXCHANGE

8.1. Dielectron

D0 performed the first dedicated experimental search for TeV^{-1} size extra dimensions at a collider [23]. They searched for effects of virtual exchanges of the KK states of the Z and γ . The signal has two distinct features: an enhancement at large masses (like in the ADD model), but also negative interference between the first KK state of the Z/ γ and the SM Drell-Yan in between the Z mass and compactification scale, as illustrated in Figure 17.

D0 searched in 200 pb^{-1} of data. The selection requirements made were the same as those in their ADD dielectromagnetic search, except that at least one of the electromagnetic clusters was required to have a matching track and no track isolation requirement was made. The data is consistent with that expected from Drell-Yan production. Limits on the compactification scale (M_C) were extracted by fitting distributions to the sum of the SM, interference, and the direct gravity templates. The lower limit on the compactification scale of the longitudinal extra dimension obtained was $M_C > 1.12 \text{ TeV}$ at the 95% confidence level. The world combined limit is currently $M_C > 6.8 \text{ TeV}$ at the 95% confidence level. More exclusive limits come from precision measurements.

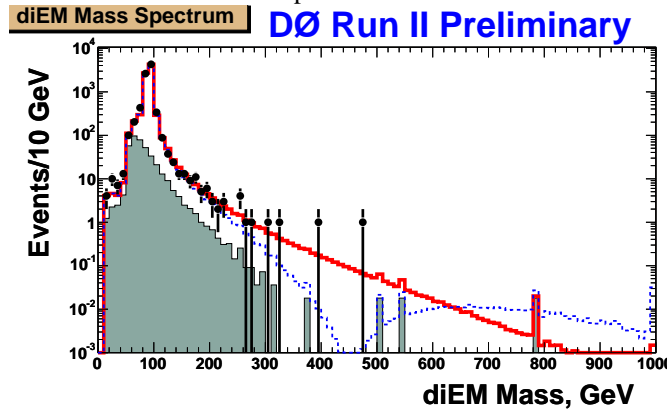


Figure 17: Invariant mass distribution obtained in D0's search for TeV^{-1} size extra dimensions. The points indicate the data distribution, the solid line the SM Drell-Yan and the dashed line the expected signal distribution for an extra dimensional signal with $\pi^2/(3M_C^2) = 5.0 \text{ TeV}^{-2}$ for 200 pb^{-1} [23].

9. FUTURE LIMITS

The present extra dimensional model limits are of the order of 1 TeV, but how far could the limits be improved in the future? Improvements are achievable at the present accelerators. There is already more data, which has been delivered to the experiments, to be analysed. For example, to date at the Tevatron approximately 400 pb^{-1} has been analysed, but over 1 fb^{-1} has been delivered to the experiments. This is to be processed and analysed. The goal is to have 4.4 to 8.5 fb^{-1} by 2009. Similarly, HERA has only used about 80 pb^{-1} to perform extra dimensional searches at present, although 200 pb^{-1} has been delivered. In addition, refinements are being made to the searches being conducted, for example neural nets are being used for particle identification, and the forward detectors are being included to increase the acceptance of searches. It has been predicted that the ADD model limits at the Tevatron could be extended from 1.28 TeV to the order of 2 TeV with 2 fb^{-1} of data and the RS model limits could be increased from 250/785 to 0.5/1 TeV for a coupling, $(k/M\text{-barPl})$ of 0.01/0.1 respectively.

But what about beyond the present experiments? The next generation of detectors are already being built. The Large Hadron Collider (LHC) at CERN is underconstruction and will operate at a center-of-mass energy of 14 TeV. This will extend the energy range accessible, enabling either new physics to be discovered or the limits to be further improved. Monte Carlo studies have been performed to predict the reaches possible at the LHC.

9.1. ADD Model Future Limits

The ADD model limits predicted are summarised in Table 6. For 2 (3) extra dimensions, they can be extended up to 9 (7) TeV in the jet+MET graviton direct emission channel with 100 fb^{-1} [24].

Table 6: Table summarising the ADD model limits from graviton emission predicted at ATLAS with low luminosity (LL) and high luminosity (HL) running for δ extra dimensions [24].

$\gamma + \text{MET}$		Jet + MET		
$M_D^{\text{MAX}} (\text{TeV})$	$\delta=2$	$M_D^{\text{MAX}} (\text{TeV})$	$\delta=2$	$\delta=3$
		LL 30 fb^{-1}	7.7	6.2
HL 100 fb^{-1}	4	HL 100 fb^{-1}	9.1	7.0

If an excess in the number of events were observed, in order to characterise the model both the gravity scale M_D and the number of extra dimensions (δ) need to be determined. Measuring the cross-section (σ) can give ambiguous results. For example, the cross-section in the case of $\delta=2$ and $M_D = 5 \text{ TeV}$ is similar to that predicted for $\delta=4$ and $M_D = 4 \text{ TeV}$. The left of Figure 18 compares the number of events/20 GeV expected in 100 pb^{-1} of ATLAS data for different values of the number of extra dimensions (δ) and gravity scale (M_D). A method to distinguish these two cases has been proposed which involves operating the collider at two different center-of-mass energies (\sqrt{s}). The predicted cross-section for 10 TeV and 14 TeV in this scenario are shown on the right of Figure 18. It has been calculated that 50 fb^{-1} of data would be needed to distinguish two cases [24].

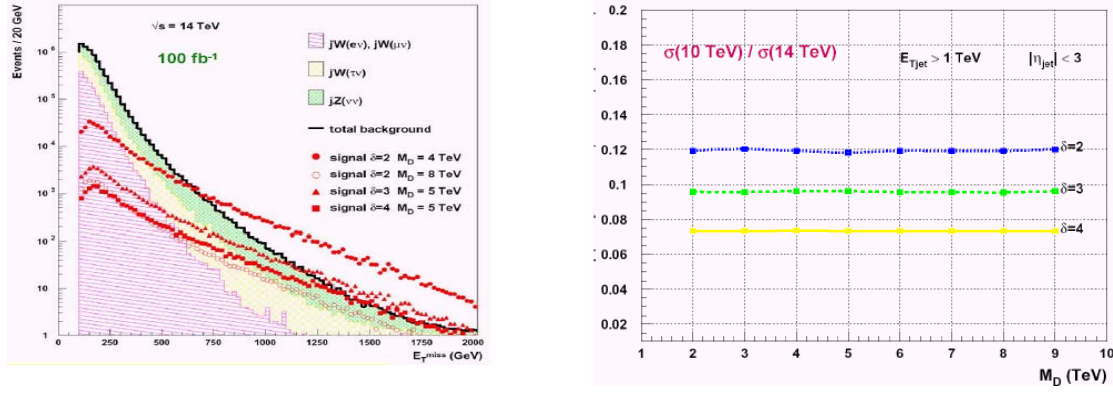


Figure 18: Left: Missing transverse energy (MET, E_T^{miss}) distribution for jets+MET channel predicted at ATLAS in the ADD model. Right: The predicted cross-section for running the LHC at 10 TeV and 14 TeV for ADD model graviton emission [24].

Using LHC virtual graviton exchange searches, it is predicted that the ADD model limits could be extended up to $\sim 6/7$ TeV with $10 \text{ fb}^{-1}/100 \text{ fb}^{-1}$. The predicted reaches for the diphoton, dilepton and combined channel are summarised in Table 7 [24].

Table 7: Summary of predicted reaches achievable using ATLAS data, for the diphoton, dilepton and the combined channel. Also shown are the predicted signal divided by background ratios (S/B) for each channel as a function of the number of extra dimensions (δ) and luminosity [24].

channel	Luminosity		$\delta = 2$	$\delta = 3$	$\delta = 4$	$\delta = 5$
$\gamma\gamma$	10 fb^{-1}	$M_s^{\text{max}}(\text{TeV})$ S/B	6.3 36/18	5.6 36/18	5.1 39/25	4.9 34/13
	100 fb^{-1}	$M_s^{\text{max}}(\text{TeV})$ S/B	7.9 50/53	7.3 62/96	6.7 55/72	6.3 51/53
$\ell\ell$	10 fb^{-1}	$M_s^{\text{max}}(\text{TeV})$ S/B	6.6 33/11	5.9 31/8	5.4 30/6	5.1 30.6
	100 fb^{-1}	$M_s^{\text{max}}(\text{TeV})$ S/B	7.9 45/48	7.5 38/21	7.0 36/16	6.6 29/6
$\gamma\gamma + \ell\ell$	10 fb^{-1}	$M_s^{\text{max}}(\text{TeV})$	7.0	6.3	5.7	5.4
	100 fb^{-1}	$M_s^{\text{max}}(\text{TeV})$	8.1	7.9	7.4	7.0

9.2. RS Model Future Limits

The RS model exclusion limits for discovery of an RS graviton as a function of the mass and curvature scale ($k/\text{M-barPl}$), predicted using data collected by the CMS detector, is shown on the left of Figure 19 [25]. With 100 fb^{-1} of LHC data the “region of interest” in this model can be completely covered. The “region of interest” is limited by the constraint of $\Lambda_\pi \leq 10 \text{ TeV}$, otherwise the model would no longer be interesting for solving the hierarchy problem and by $k/\text{M-barPl} < 0.1$ for low-energy consistency. Note that the diphoton channel is more exclusive than the electron and muon channels. Investigations in to how to distinguish the RS model graviton from other new physics scenarios have also been performed. A resonance observed in the dielectron channel could be caused by a Z' boson, which has a spin of 1, or a RS model graviton, which has a spin of 2. The two cases could be potentially be discriminated by studying the angular distribution, as illustrated on the right of Figure 20 [5].

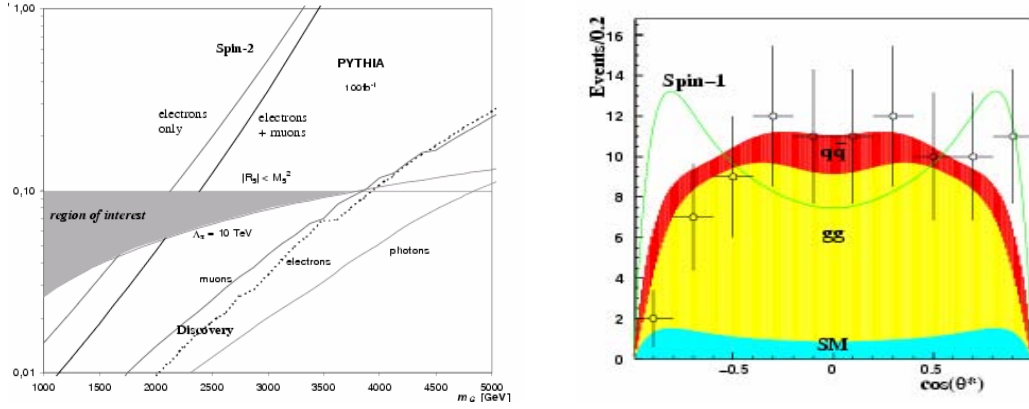


Figure 19: Left: The RS model exclusion limits for discovery of an RS graviton as a function of the mass and curvature scale (k/\bar{M}_{Pl}), predicted using data collected by the CMS detector [25]. Right: Angular distribution of e^+e^- pairs for an RS model graviton resonance of mass 1.5 TeV at ATLAS with 100 fb^{-1} data (open circles), the gg dominant production (yellow curve), the SM (bottom blue curve) and the expected distribution for a spin 1 resonance (green line) [5].

9.3. TeV^{-1} Size Extra Dimensional Future Limits

It has been predicted that at ATLAS it would be possible to detect a resonance in the lepton-lepton invariant mass spectrum of up to an energy of 5.8 TeV with 100 fb^{-1} , and if no peak is observed with an integrated luminosity of 300 fb^{-1} a limit on the compactification scale (M_C) of less than 12-13.5 TeV could be achieved [7]. Figure 20 shows the predicted invariant mass distribution for a compactification scale of 4 TeV for dielectrons and dimuons. The width of an observed resonance would depend on the resolution of the detectors. The resolving power for electrons at ATLAS is predicted to be better than that for muons, as illustrated in the figure. This shows an optimistic resolution of $\Delta E/E \sim 0.7$ for 2 TeV electrons and approximately 20% for muons. Investigations have also been made into methods to distinguish TeV^{-1} size extra dimensional model resonances from other models (M_2 , Z' , RS graviton) which predict resonances by studying the forward-backward asymmetries, as demonstrated in Figure 21 [7].

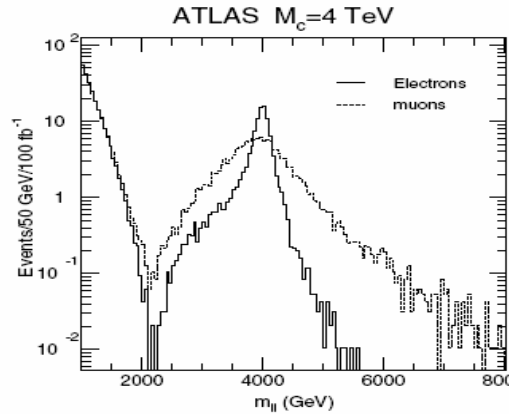


Figure 20: Invariant mass distribution of dileptons for electrons (full line) and muons (dashed line) in the presence of TeV^{-1} size extra dimensions with a compactification scale of 4 TeV predicted at ATLAS. The distribution assumes the mass of the lowest lying KK excitation to be 4 TeV [7].

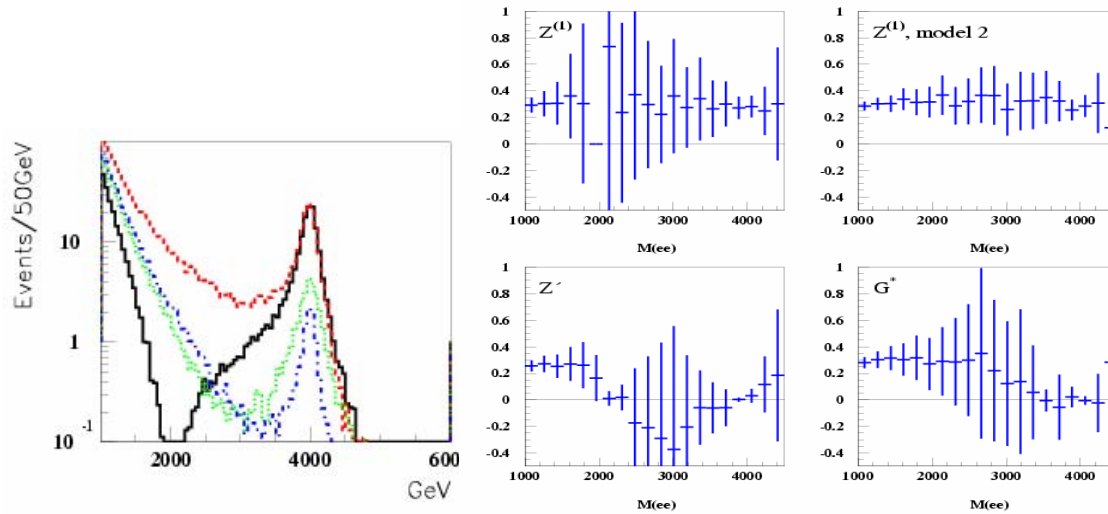


Figure 21: Invariant mass distribution (left) and measured forward-backward asymmetries (right) predicted at the LHC in the dielectron channel for different types of 4 TeV resonances: M1 TeV^{-1} extra dimensional model ($Z^{(1)}/\gamma^{(1)}$), M2 TeV^{-1} extra dimensional model, Z' and G^* [7].

10. CONCLUSION

The data distributions observed in searches for extra dimensions performed at accelerators presented in this lecture were found to be consistent with those expected from the SM. The data have been used to set limits on the ADD, RS and TeV^{-1} size extra dimensional models, and are of the order of 1 TeV. These analyses are being updated and refined, so in the future these limits are likely to be improved. In addition, an increasing number of channels are being used to search for extra dimensions at accelerators. For example, at the Tevatron, searches are also underway in the $\tau\tau$, jet-jet and ZZ channels. In the future, data from the LHC will enable searches probe up to $\sim 5\text{-}7$ TeV with 100 fb^{-1} .

Acknowledgments

The author would like to thank Joanne Hewett for the invitation to present this guest lecture at SLAC and also to acknowledge and thank PPARC for its support in the form of a PPARC Postdoctoral Fellowship.

References

- [1] N. Arkani-Hamed, S. Dimopoulos and C. Dvali, "The Hierarchy Problem And New Dimensions At A Millimeter", Phys. Lett. B429, 261 (1998).
- [2] L. Randall and R. Sundrum, "An Alternative To Compactification", Phys. Rev. Lett. 83: 4690-4693 (1999) (hep-th/9906064).
- [3] I. Antoniadis, "A Possible New Dimension at a few TeV," Phys. Lett. B246:377-384 (1990).
- [4] J. Hewett, "Indirect Collider Signals For Extra Dimensions", Phys. Rev. Lett. 82:4765-4768 (1999) (hep-ph/9811356).
- [5] B. Allanach, K. Odagiri, M. Palmer, M. Parker, A. Sabetfakhri, B. Webber, "Exploring Small Extra Dimensions At The Large Hadron Collider", JHEP 0212:039 (2002) (hep-ph/0211205).
- [6] H. Davoudiasl, J. Hewett and T. Rizzo, Phys. Rev. D63:075004 (2001). (hep-ph/0006041).

- [7] G. Azuelos and G. Polesello, "Prospects For The Detection Of Kaluza-Klein Excitations Of Gauge Bosons In The Atlas Detector At The LHC", *Eur.Phys.J.C39S2*:1-11 (2005).
- [8] <http://www.fnal.gov/>
- [9] <http://www.desy.de/html/home/>
- [10] <http://public.web.cern.ch/Public/Welcome.html>
- [11] The ALEPH, DELPHI, L3, OPAL Collaboration and the LEP Exotica Working Group, LEP Exotica WG 2004-03, ALEPH 2004-007 PHYSICS 2004-006, DELPHI 2004-033 CONF 708, L3 Note 2798.
- [12] CDF Collaboration, D. Acosta *et al.*, "Limits On Extra Dimensions And New Particle Production In The Exclusive Photon And Missing Energy Signature In P Anti-P Collisions At $S^{**}(1/2) = 1.8\text{-TeV}$ ", *Phys. Rev. Lett.* 89:281801 (2002) (hep-ex/0205057).
- [13] G. Giudice, R. Rattazi and J. Wells, *Nucl. Phys. B544*: 3-38 (1999) (hep-ph9811291).
- [14] CDF Collaboration, D. Acosta *et al.*, "Search for Kaluza-Klein Graviton Emission In p anti-p Collisions At $\sqrt{s} = 1.8\text{ TeV}$ Using The Missing Energy Signature", *Phys. Rev. Lett.* 92, 121802 (2003).
- [15] D0 Collaboration, V.M. Abazov *et al.*, "Search for Large Extra Dimensions In The Monojets + Missing ET Channel With The D0 Detector", *Phys. Rev. Lett* 90: 251802 (2003) (hep-ex/0302014).
- [16] D0 Collaboration, "Search For Large Extra Spatial Dimensions In Jets + Missing ET Topologies", D0CONF 4440 v1.4 (March 2004).
- [17] CDF Collaboration (A. Abulencia *et al.*), "Search For New High Mass Particles Decaying To Lepton Pairs In P Anti-P Collisions At $S^{**}(1/2) = 1.96\text{-TeV}$ ", hep-ex/0507104 (2005).
- [18] D0 Collaboration, "Search For Large Extra Dimensions In The Dielectron And Diphoton Channels With 200 pb⁻¹ Of Run II Data", D0 Note 4336-Conf, (2/25/04).
- [19] D0 Collaboration (V.M. Abazov *et al.*), "Search For Large Extra Spatial Dimensions In Dimuon Production At D0", hep-ex/0506063 (June 2005).
- [20] D0 Collaboration (V.M. Abazov *et al.*), "Search For Randall-Sundrum Gravitons In Dilepton And Diphoton Final States", *Phys.Rev.Lett.*95:091801(2005) (hep-ex/0505018).
- [21] http://www-cdf.fnal.gov/physics/exotic/r2a/20040805.diphoton_rsgrav/
- [22] H1 Collaboration, (C. Adloff *et al.*). "Search For New Physics in e⁺/-q Contact Interactions At HERA", DESY 03-052 May 2003 *Phys.Lett.B568*:35-47 (2003) (hep-ex/0305015).
- [23] D0 Collaboration, "Search For Large and TeV⁻¹ Extra Dimensions In The Dielectron Channel With 200 pb⁻¹ Of Data", D0 Note 4349-Conf (17 March 2004).
- [24] Talk presented by Ambreesh Gupta, "Search For Extra Dimensions at ATLAS", at PASCOS 2003 (3-8 January 2003).
- [25] ATLAS Collaboration and CMS Collaboration, "Search For Extra Dimensions At LHC", *Eur.Phys.J.C33*:S924-S926 (2004) (hep-ex/0310020).